Behavior of Catalytic Pellets at High Reaction Rates. The Effect of Edges

Sergio D. Keegan,[†,‡] Néstor J. Mariani,[†,‡] Osvaldo M. Martínez,[†,‡] and Guillermo F. Barreto*[,†,‡]

Departamento de Ingeniería Química, Facultad de Ingeniería, and Centro de Investigación y Desarrollo en Ciencias Aplicadas "Dr. J. J. Ronco" (CINDECA), CONICET, Universidad Nacional de La Plata, Calle 47 No. 257, CP B1900AJK, La Plata, Argentina

The diffusion and reaction problem in catalytic pellets of any shape subject to diffusive transport limitations is undertaken in this contribution. Effective reaction rates in three-dimensional (3D) catalysts can be evaluated through a series solution written in terms of powers of $(1/\Phi)$ when strong diffusion limitations are present. In a recent paper, Keegan et al. [*Chem. Eng. J.* **2005**, *110*, 41] have clearly demonstrated for smooth catalysts that the second-order term [in $(1/\Phi)^2$] depends essentially on the shape of the pellet. In this context, the purpose of this paper is to develop expressions of the second-order term for two-dimensional (2D) or 3D catalytic bodies showing edges. While the first-order term allows definition of the proper *size* of a catalyst, the second-order term provides a characterization for the *shape* of the catalyst. The possibility of using this characterization of catalyst shape in a geometrical one-dimensional (1D) model to approximate the behavior of given 2D or 3D pellets is analyzed. Also, the direct use of the two-term truncated series for complementing the numerical evaluation of the conservation equation is described.

1. Introduction

Diffusive transport in most kinds of commercial catalytic pellets proceeds along more than one spatial coordinate. The general case will be a three-dimensional (3D) problem, while two-dimensional (2D) problems will be frequent [The term "3D" means that no suitable coordinate system can be chosen to reduce the number of coordinate directions taken by the flux of reactants from 3. 1D or 2D applies when either 1 or 2 suitable coordinate directions can be found (e.g., axisymmetric problems will be 2D and problems on a sphere will be 1D).], mainly due to axisymmetry, and will also apply for monolith reactors with a catalytic coating on noncircular channels.[2]

As discussed in recent contributions,[1,3,4] in practical applications it will be convenient to avoid 2D or 3D computations by employing some kind of approximation to the actual problem. This is feasible largely because it is a well-known fact that if different catalytic bodies are compared in terms of the characteristic length, $l = V_p/S_p$, the effect of shape is tempered. Table 1 shows deviations between the effectiveness factors in a one-dimensional (1D) slab (the simplest 1D geometry) and in a finite circular cylinder (a 2D problem) compared at the same l for different kinetics (a precise definition of $r(Y)$ is given in the next section).

If the actual problem is that of the cylinder, Table 1 shows that the correct order of magnitude is provided by the slab, but it is evident that the deviations warrant the search for a better approximation. Even more uncertain results can be expected when multiple reactions take place. Thus, the data in Table 1 suggest that the effect of shape cannot be ignored and that, in order to avoid 2D or 3D calculations without loosing accuracy, the 1D analogue (or any other kind of approximation) will have to be defined on the basis of sensible criteria. It seems obvious that these criteria should involve a geometrical characterization of the actual catalyst.

Table 1. Maximum Relative Difference (Δ) between the Effectiveness Factors of a Slab (1D) and a Circular Cylinder with a Height/Radius Ratio of 1.7 (2D), Compared at the Same *l*

$r(Y)$	Y^2	Y	$Y^{1/2}$	1 (if $Y > 0$)	$36Y/(1+5Y)^2$
Δ (%)	18	19	22	34	38

The analysis of the behavior at high reaction rates can provide a geometrical characterization of a given catalyst. For the case of a single reaction and uniform activity on 1D catalysts (see, e.g., refs 4−6), the effectiveness factor η for high values of the Thiele modulus Φ can be expressed as

$$\eta = \frac{\mathcal{I}_1}{\Phi} - \frac{\mathcal{I}_2}{\Phi^2}\Gamma + ... \qquad (1.a)$$

$$\Gamma = \frac{\sigma}{\sigma + 1} \qquad (1.b)$$

where $\mathcal{I}_1$ and $\mathcal{I}_2$ are coefficients depending on the type of kinetic law (all quantities in eqs 1 will be precisely defined in the next section) and $\sigma = (0, 1, \text{and } 2)$ for a slab, a long circular cylinder, and a sphere, respectively.

For very fast reactions, eq 1.a can be truncated to $\eta = \mathcal{I}_1/\Phi$, a very well-known expression (see, e.g., ref 7) corresponding to conditions that will be identified here as the *limiting regime*. The second-order term in eq 1.a is characterized by the coefficient Γ that depends on the shape of the catalyst, eq 1.b. Conditions under which the two-term expression (eq 1.a) applies (i.e., for reaction rates not necessarily as high as those for the limiting regime) will be identified as the *asymptotic regime*. Recently, Keegan et al.[1] expressed Γ for 2D or 3D catalysts restricted to geometries showing smooth external surfaces. The effect of activity gradients was also included in that contribution.

If a 1D geometrical model with adjustable parameters is intended as an approximation to avoid 2D or 3D calculations, a reasonable criterion can be stated by forcing the model to show the same behavior as the actual particle at large values of Φ. This can be done in practice if both, the model and the actual particle, present the same value of Γ.

The main purpose of this paper is to develop a general expression of Γ for catalyst geometries showing edges, extending

* To whom correspondence should be addressed. E-mail: barreto@quimica.unlp.edu.ar.

† Departamento de Ingeniería Química.

‡ Centro de Investigación y Desarrollo en Ciencias Aplicadas "Dr. J. J. Ronco" (CINDECA).

10.1021/ie050740m CCC: $33.50
Published on Web 12/06/2005

in this way the results presented by Keegan et al.[1] This task includes the development of restrictions for the validity of the two-term truncated series (eq 1.a). Actually, except for the case of spherical particles, practically all types of commercial pellets are finite cylinders (of different cross-sectional shapes) and, therefore, show edges at the intersections of the bases and the cylindrical envelope. In addition, multilobe pellets also show longitudinal edges.

The two-term truncated series (eq 1.b) constitutes an approximation for η that can be used for complementing the numerical solution of 2D or 3D conservation equations: a numerical algorithm can be used for low values of Φ, and the truncated series can be used at large values of Φ, when steep (and difficult to evaluate) solutions take place. This application and the potential use of Γ as a shape factor will be discussed and exemplified.

For the most part, a single catalytic reaction will be assumed. However, arguments will be given to show that the significance of the present contribution can be extended to the very important case of multiple-reaction systems.

2. Problem Statement

Although a catalytic pellet will be frequently invoked, the treatment in this and following sections can be directly extended to catalytic coatings on structured devices. A single catalytic reaction, with the following restrictions, will be considered: (a)- *Uniform composition and temperature exist at the permeable part of the catalyst external surface (S_p).* (b) *Constitutive equations for the fluxes (transport model) are isotropic and intrinsically independent of position inside the catalyst*.

It was discussed by Keegan et al.[1] that these conditions allow employing a single state variable to represent the system. As such, a dimensionless variable Y is defined by

$$Y = \frac{1}{\mathscr{J}_A}\int_{C_{Ae}}^{C_A} D(C_A)\, dC_A \tag{2.a}$$

$$\mathscr{J}_A = \int_{C_{Ae}}^{C_{AS}} D(C_A)\, dC_A \tag{2.b}$$

where C_A is the molar concentration of a key reactant A, C_{AS} is the value of C_A on S_p and C_{Ae} is the value of C_A when chemical equilibrium is reached inside the pellet. $D(C_A)$ is such that the flux of A can be expressed as $\mathbf{N}_A = -D(C_A)\,\nabla\, C_A$, after taking into account the relations between C_A and the remaining molar concentrations and temperature, which arise by combining the mass and energy conservation balances.[1] The conservation balance for species A is then written in terms of Y,

$$\mathscr{L}(Y) = \frac{1}{\lambda^2} a(\mathbf{x})\, r(Y) \text{ in } V_p \tag{3.a}$$

$$Y = 1 \text{ on } S_p \tag{3.b}$$

$$\nabla Y = 0 \text{ on } S_N \tag{3.c}$$

where $\mathscr{L}$ is the Laplacian and the *global reaction scale* λ is defined by

$$\lambda^2 = \mathscr{J}_A/\pi_{AS} \tag{3.d}$$

The dimensionless reaction rate in eq 3.a is defined by $r(Y) = \pi_A(Y)/\pi_{AS}$, where π_A is the net consumption rate of A and π_{AS} is its value at S_p. Note that $r(1) = 1$ on S_p and, according to eq 2.a, $Y = 0$ when $C_A = C_{Ae}$; hence, $r(0) = 0$.

The activity a, a function of the spatial coordinate vector $\mathbf{x} = (x_1, x_2, x_3)$, is normalized according to

$$\frac{1}{V_p}\int_{V_p} a(\mathbf{x})\, dV = 1 \tag{3.e}$$

S_p stands for the permeable parts, and S_N stands for the sealed parts (inaccessible to reactants) of the V_p boundary. (The symbol V_p will stand for both the spatial domain corresponding to the catalyst and its volume. Similarly, S_p stands for the domain of the permeable external surface and for its area.)

It will be assumed that the activity at any point on S_p is finite but not necessarily uniform.

3. Asymptotic Behavior at High Reaction Rates

It was shown by Keegan et al.[1] that, for a catalytic body showing a smooth surface S_p, eq 3.a can be reduced to the following asymptotic form at low enough values of λ,

$$\frac{d^2Y}{d\zeta^2} - \lambda_S T_S \frac{dY}{d\zeta} = (1 - 2\zeta\lambda_S \mathscr{A}_S) r(Y) \tag{4.a}$$

with the boundary conditions

$$\zeta = 0: \quad Y = 1 \tag{4.b}$$

$$\zeta \to \infty: \quad Y \to 0, \quad (dY/d\zeta) \to 0 \tag{4.c}$$

Equation 4.a applies at each point on S_p (local basis). To describe the symbols, let a_S be the local value of a on S_p and ξ_n be the coordinate along the local normal to S_p, increasing inwardly and with the origin at S_p. Then, $\lambda_S = \lambda/a_S^{1/2}$ is the *local reaction scale* and $\zeta = \xi_n/\lambda_S$ is the *stretched coordinate*. Also, $(T_S/2)$ is the local *average curvature* that can be expressed in terms of the principal radii of curvature R_a and R_b as

$$T_S = \frac{1}{R_a} + \frac{1}{R_b} \tag{5}$$

R_i (i = a, b) is positive if the center of curvature is inwardly oriented and negative otherwise. [For a point P on a surface, assume the normal unit vector $\mathbf{n}$ is identified. Then, a *normal plane* at P is any plane containing $\mathbf{n}$ (there is a bundle of such planes), a *normal section* at P is a curve resulting from intersection of the surface and a normal plane, a *normal curvature* is the curvature of a normal section at P, a *principal curvature* is either the minimum or the maximum normal curvature, and a *radius of curvature* is the inverse of a normal curvature.] Finally,

$$\mathscr{A}_S = -\frac{a'_S}{2a_S} \tag{6.a}$$

$$a'_S = (\partial a/\partial \xi_n)|_{\xi_n=0} \tag{6.b}$$

The primary conditions for eqs 4 to hold at each point of S_p are[1]

$$\lambda_S \ll \min\{|R_a|, |R_b|\} \tag{7.a}$$

$$\lambda_S \ll a_S/|a'_S| \tag{7.b}$$

$$\lambda_S \ll d \tag{7.c}$$

where d is the thickness of the pellet in the local normal direction.

Restriction 7.c is necessary for the boundary condition of eq 4.c to apply; that is, the catalyst can be considered to be much

deeper than the distance (penetration depth) needed to approach equilibrium conditions ($Y = 0$, $dY/d\zeta = 0$). It can be shown that the penetration depth χ in the asymptotic regime is of the same order of magnitude as λ_S.

The edges on the external surface can be described as the boundaries between *smooth sectors* showing continuous curvature properties. If values of χ are smaller than the linear dimensions of those sectors, it becomes clear that the effect of edges will be circumscribed to small zones around them, where the concentration fields from two sectors become overlapped. In this case, the main contribution to the overall rate of mass transfer will be that obtained by using the previous formulation for the whole surface of each sector, as if the edges were absent. Accordingly, the solution obtained for eqs 4, as given by Keegan et al.,[1] can be used for the local flux on each sector

$$N_{AS,high} = -\frac{\mathcal{J}_A}{\lambda_S}\left(\frac{dY}{d\zeta}\right)_{\zeta=0} = \frac{\mathcal{J}_A}{\lambda}[\mathcal{I}_1 a_S^{1/2} - \mathcal{I}_2\lambda(T_S + \mathcal{A}_S)] \quad (8)$$

where

$$\mathcal{I}(Y_0) = 2\int_0^{Y_0} r(Y)\, dY \quad (9.a)$$

$$\mathcal{I}_1 = [\mathcal{I}(1)]^{1/2} \quad (9.b)$$

$$\mathcal{I}_2 = \frac{1}{\mathcal{I}_1}\int_0^1 [\mathcal{I}(Y_0)]^{1/2}\, dY_0 \quad (9.c)$$

By integration of eq 8 over the surface S_j of each sector j, the amount of moles of A transferred per unit time will be

$$M_{high,j} = \mathcal{J}_A\left[\frac{1}{\lambda}\mathcal{I}_1\int_{S_j} a_S^{1/2}\, dS - \mathcal{I}_2\int_{S_j}(T_S + \mathcal{A}_S)\, dS\right] \quad (10)$$

It is worth stressing that the terms associated with curvature effects and activity gradients (T_S and $\mathcal{A}_S$) in eqs 4.a, 8, and 10 are of a second order of magnitude, due to the relatively low values imposed by restrictions 7.a and 7.b to λ_S.

Next, a correction to eq 10 will be developed to account for the effect of the edges.

3.1. The Contribution of Edges. In this section, we deal with edges between two smooth sectors belonging to S_p, while cases involving S_N will be considered in section 5.

We should first recall that if in eq 4.a the terms depending on T_S and $\mathcal{A}_S$ are ignored, the conservation balance for the limiting regime is obtained

$$d^2Y_0/d\zeta^2 = r(Y_0) \quad (11.a)$$

$$\zeta = 0: \quad Y_0 = 1 \quad (11.b)$$

$$\zeta \to \infty: \quad Y_0 \to 0, \quad (dY_0/d\zeta) \to 0 \quad (11.c)$$

where the suffix "0" identifies the limiting regime. Equation 11.a can be rewritten as

$$dY_0/d\zeta = -\mathcal{I}(Y_0)^{1/2} \quad (12)$$

with $\mathcal{I}(Y_0)$ given in eq 9.a. From eq 12, the flux at the surface is given by

$$N_{AS,0} = -\frac{\mathcal{J}_A}{\lambda_S}\left(\frac{dY_0}{d\zeta}\right)_{\zeta=0} = \frac{\mathcal{J}_A}{\lambda_S}\mathcal{I}_1 \quad (13)$$

which is the dominant term in eq 8.

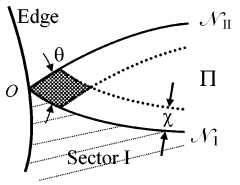

Figure 1. Perspective of the region close to an edge. Π is the plane normal to the edge at point *O*. $\mathcal{N}_I$ and $\mathcal{N}_{II}$ are normal sections defined by the intersections between Π and the smooth sectors I and II.

Equation 12 can now be used to obtain an approximate expression for the penetration depth χ, which can be defined as the distance from S_p at which $r(Y)$ reaches a residual value $r(Y^*) = 0.1$,

$$\chi = \lambda_S\int_{Y^*}^1 \mathcal{I}(Y)^{-1/2}\, dY \quad (14)$$

The exact value of the integral in eq 14 depends on the form of $r(Y)$, but it does not rise above a few units (e.g., for $r = Y^{1/4}$, $\chi = 2.04\lambda_S$; for $r = Y$, $\chi = 2.3\lambda_S$; and for $r = Y^2$, $\chi = 1.9\lambda_S$). As quoted before, both χ and λ_S are of the same order of magnitude.

Now, we have presented the necessary elements for a conceptual description of the effect of edges. Consider two smooth sectors (I, II) that intersect defining an edge. Let Π be the plane normal to the edge at a generic point *O* belonging to it. This plane is also a normal plane for both sectors at point *O* and defines two normal sections ($\mathcal{N}_I$ and $\mathcal{N}_{II}$), as depicted in Figure 1. The tangents of $\mathcal{N}_I$ and $\mathcal{N}_{II}$ at the edge define the intersection angle θ. From $\mathcal{N}_I$ and $\mathcal{N}_{II}$ and over the plane Π, we can identify the strips of width χ where the catalytic reaction takes place. Both strips interpenetrate in the dashed region close to the edge, as shown in Figure 1.

It is evident that, by integrating the flux over both sectors independently of each other just up to the edge (as done for eq 10), the region of interpenetration is, up to some extent, considered twice: for the reaction of the reactants incoming from sector I and from sector II. To estimate the correction to eq 10, an amount proportional to the moles transferred from one of the sectors should be discounted.

The portion of each sector involved in the interpenetration region will present a width, whose order of magnitude will be that of χ, and a length, which will be that of the edge, W_k ("k" is the suffix to denote a generic edge). It follows that an order of magnitude estimate of the correction to eq 10 will be ($W_k\chi N_{AS}$). Employing $N_{AS,0}$ (eq 13) for N_{AS} and eq 14 for χ, we obtain

$$[\Delta M]_k \sim W_k\mathcal{J}_A\mathcal{I}_1\int_{Y^*}^1 \mathcal{I}(Y)^{-1/2}\, dY \quad (15)$$

Equation 15 suggests that the correction $[\Delta M]_k$ does not depend on λ or on the catalytic activity field, as a first approximation, when small values of λ are considered. In other words, if a series expansion for $[\Delta M]_k$ in powers of λ is envisaged, the leading term will be independent of λ and of the activity field. As a consequence, it will be comparable with the contribution $\mathcal{J}_A\mathcal{I}_2\int_{S_j}(Y_S + \mathcal{A}_S)\, dS$ in eq 10. The leading term of $[\Delta M]_k$, denoted as $[\Delta M_{high}]_k$, is what we need to complete the formulation of M_{high}.

Accordingly, we will develop in the following paragraphs an appropriate expression for $[\Delta M_{high}]_k$, based on a geometrical simplification and assuming uniform activity. However, this treatment does not allow one to visualize the restrictions that should be imposed on values of λ for being considered "small enough", i.e., restrictions that play the role of inequalities (7.a

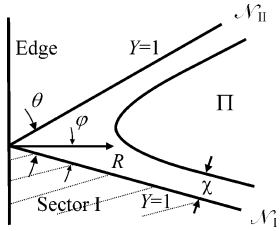

Figure 2. Sketch of the straight wedge.

and 7.b), but for the edge zones. This issue is covered in detail in the Supporting Information for this paper, and the whole body of restrictions for the asymptotic regime to apply will be summarized in the next section.

To find out an expression for $[\Delta M_{high}]_k$, we should realize that, at a given point of an edge, the local field of Y on the plane Π (Figure 1) will be largely determined by the dihedral angle θ defined by the tangents of $\mathcal{N}_I$ and $\mathcal{N}_{II}$ at the edge. Then, the approximation of the local field can be evaluated by considering a straight wedge with a very long edge and faces (sectors) and, hence, geometrically defined just by the dihedral angle θ, as depicted in Figure 2. Besides, it will be assumed that the activity in the straight wedge is uniform and equal to a certain value a_w (it will be shown later that ΔM_{high} does not effectively depend on this quantity).

As the wedge is assumed to be very long, we can ignore variations of Y in the direction parallel to the edge. Then, by using polar coordinates (see Figure 2), the conservation balance is written

$$\frac{\partial}{R\,\partial R}\left(R\,\frac{\partial Y}{\partial R}\right)+\frac{1}{R^2}\frac{\partial^2 Y}{\partial \varphi^2}=\frac{1}{{\lambda_w}^2}r(Y) \tag{16}$$

where $\lambda_w = \lambda/{a_w}^{1/2}$ is the local reaction scale defined with the constant value of activity a_w.

Introducing the "stretched" radial coordinate $\rho = R/\lambda_w$ in eq 16,

$$\frac{\partial}{\rho\,\partial \rho}\left(\rho\,\frac{\partial Y}{\partial \rho}\right)+\frac{1}{\rho^2}\frac{\partial^2 Y}{\partial \varphi^2}=r(Y);\quad \rho \geq 0,\quad 0 \leq \varphi \leq \theta \tag{17.a}$$

As sectors I and II are assumed to extend boundlessly, the appropriate boundary conditions are (see Figure 2)

$$Y = 1 \text{ at } \varphi = 0 \text{ and } \varphi = \theta \tag{17.b}$$

$$Y = 1 \text{ at } \rho = 0;\quad Y = 0 \text{ if } \rho \to \infty \text{ and } 0 < \varphi < \theta \tag{17.c}$$

The penetration of the key species will look like what is sketched in Figure 2, where we can appreciate that far from the edge the penetration depth corresponds to that of a flat sector. Therefore, recalling that the activity is uniform, far enough from the edge, the flux at the surface corresponds to that in eq 8 with $(T_S + \mathcal{A}_S) = 0$, which is the same as the value for the limiting regime, expressed in eq 13,

$$N_{AS,far} = \frac{\mathcal{J}_A}{\lambda_w}\mathcal{I}_1$$

Let us assume now that eqs 17 have been solved and the normal derivative at $\varphi = 0$, $(1/\rho)(\partial Y/\partial \varphi)_{\varphi=0}$, has been evaluated. The local flux at sector I is expressed as

$$N_{AS,wedge} = -\frac{\mathcal{J}_A}{\lambda_w}\frac{1}{\rho}(\partial Y/\partial \varphi)_{\varphi=0}$$

Then, the local correction for sector I can be expressed as $\Delta N_{AS} = N_{AS,wedge} - N_{AS,far}$:

$$\Delta N_{AS} = -\frac{\mathcal{J}_A}{\lambda_w}\frac{1}{\rho}(\partial Y/\partial \varphi)_{\varphi=0} - \frac{\mathcal{J}_A}{\lambda_w}\mathcal{I}_1$$

Because of symmetry, exactly the same value of ΔN_{AS} will also hold for sector II. The overall correction per unit length of the wedge can be obtained by integrating $(2\Delta N_{AS})$ over the radial variable R up to a certain radius, R_∞, large enough for ΔN_{AS} to become essentially nil. Then,

$$\frac{\mathrm{d}(\Delta M_{high})}{\mathrm{d}W} = 2\int_0^{R_\infty}\Delta N_{AS}\,\mathrm{d}R = 2\lambda_w\int_0^{\infty}\Delta N_{AS}\,\mathrm{d}\rho$$

The stretched radial coordinate ρ has been introduced in the third term. In practice, values of ρ needed for ΔN_{AS} to become nil are of only a few units (the upper limit taken as ∞ is adopted for the sake of definiteness). By expliciting ΔN_{AS}, we finally express

$$\frac{\mathrm{d}(\Delta M_{high})}{\mathrm{d}W} = -\mathcal{J}_A\mathcal{I}_2\omega(\theta) \tag{17.d}$$

$$\omega(\theta) = \frac{2}{\mathcal{I}_2}\int_0^{\infty}\left[\frac{1}{\rho}(\partial Y/\partial \varphi)_{\varphi=0} + \mathcal{I}_1\right]\mathrm{d}\rho \tag{17.e}$$

where the coefficient $\mathcal{I}_2$ (eq 9.c) that depends on the form of $r(Y)$ is introduced as a matter of convenience. It will be understood throughout this paper that the definition of $\omega(\theta)$ (eq 17.e) is associated with the solution of eqs 17.a−c. Although only the dependence of ω on θ is made explicit, it should be recalled that ω will also depend on the form of $r(Y)$.

Equation 17.d accounts for the correction along an elementary length $\mathrm{d}W$, at which θ is regarded as being essentially constant. To evaluate the correction $[\Delta M_{high}]_k$ over the whole length W_k of the edge, eq 17.d should be integrated, accounting for possible variations of the angle θ. Then,

$$[\Delta M_{high}]_k = -\mathcal{J}_A\mathcal{I}_2\int_{W_k}\omega(\theta)\,\mathrm{d}W \tag{18}$$

As was previously pointed out, ΔM_{high} does not depend on a_w (eqs 17.e and 18).

By adding eq 10 applied to all sectors in which S_p is assumed to be decomposed and eq 18 for the total number of edges, we obtain for M_{high}

$$M_{high} = \frac{\mathcal{J}_A}{\lambda}S_p\{\mathcal{I}_1({a_S}^{1/2})_{av} - \lambda\mathcal{I}_2[(T_S + \mathcal{A}_S)_{av} + \Omega_{av}]\} \tag{19.a}$$

where

$$({a_S}^{1/2})_{av} = {S_p}^{-1}\sum_j[{a_S}^{1/2}S]_j \tag{19.b}$$

$$[{a_S}^{1/2}S]_j = \int_{S_j}{a_S}^{1/2}\,\mathrm{d}S \tag{19.c}$$

$$(T_S + \mathcal{A}_S)_{av} = {S_p}^{-1}\sum_j[(T_S + \mathcal{A}_S)S]_j \tag{19.d}$$

$$[(T_S + \mathcal{A}_S)S]_j = \int_{S_j}(T_S + \mathcal{A}_S)\,\mathrm{d}S \tag{19.e}$$

$$\Omega_{av} = {S_p}^{-1}\sum_k[\omega W]_k \tag{19.f}$$

$$[\omega W]_k = \int_{W_k}\omega\,\mathrm{d}W \tag{19.g}$$

By defining $\mathbb{R} = \mathscr{I}_2/\mathscr{I}_1$, the *characteristic length* of the catalyst $l = V_p/S_p$, and

$$\Gamma = \frac{l}{(a_S^{1/2})_{av}}[(T_S + \mathscr{A}_S)_{av} + \Omega_{av}] \tag{19.h}$$

we can alternatively write for M_{high}

$$M_{high} = \frac{\mathscr{I}_A S_p (a_S^{1/2})_{av} \mathscr{I}_1}{\lambda}\left[1 - \mathbb{R}\frac{\lambda}{l}\Gamma\right] \tag{20.a}$$

Employing the usual definition of the effectiveness factor $\eta = M/(\pi_{As} V_p)$ and the Thiele modulus $\Phi^2 = (l/\lambda)^2 = l^2\pi_{As}/\mathscr{I}_A$,

$$\eta_{high} = \frac{\mathscr{I}_1 (a_S^{1/2})_{av}}{\Phi}\left(1 - \frac{\mathbb{R}}{\Phi}\Gamma\right) \tag{20.b}$$

For the case of uniform activity, i.e., $a = 1$,

$$(a = 1) \qquad \eta_{high} = \frac{\mathscr{I}_1}{\Phi}\left(1 - \frac{\mathbb{R}}{\Phi}\Gamma\right) \tag{21.a}$$

$$\Gamma = l[(T_S)_{av} + \Omega_{av}] \tag{21.b}$$

Equations 19−21 constitute the main results of this paper. In essence, the formulation for Γ (eq 19.h) allows the evaluation of M or η for short λ (or high Φ) up to a second order of magnitude.

Comparing eq 19.h for Γ with the corresponding expression developed by Keegan et al.[1] for smooth surfaces, it is easy to recognize that the former just adds the term Ω_{av} due to the effect of the edges.

4. Constraints and Limitations for the Use of Equations 19−21

Constraints on the value of λ arise from the analysis of smooth sectors[1] and from the treatment of edges. They involve curvatures of S_p, activity gradients at S_p, and some specific dimensions of the catalyst body. Equations 7.a−c are the relevant restrictions for the smooth sectors.

Two restrictions, holding at each point of an edge and concerning the curvature effects, arise from the analysis in the Supporting Information for this paper,

$$\lambda_w\left|\frac{1}{R_{C,I}} + \frac{1}{R_{C,II}}\right| \ll 1 \tag{22.a}$$

$$\frac{\lambda_w}{3\theta}\left|\frac{1}{R_{\mathcal{N},I}} + \frac{1}{R_{\mathcal{N},II}}\right| \ll 1 \tag{22.b}$$

where $\lambda_w = \lambda/a_w^{1/2}$, a_w is the activity at the edge, $R_{\mathcal{N},I}$ is the radius of curvature of $\mathcal{N}_I$ at the edge, and $R_{C,I}$ is the radius of curvature of the normal section C_I perpendicular to $\mathcal{N}_I$ at the edge (i.e., in the same direction of the edge); all quantities are defined on a local basis. (At the given point of the edge, its osculating plane will not be, in general, normal to any of both sectors; then, the radius of curvature of the edge will not, in general, coincide with either $R_{C,I}$ or $R_{C,II}$.) Similar definitions apply for $R_{\mathcal{N},II}$ and $R_{C,II}$.

When expression 22.a is satisfied, the assumption of negligible variations of Y in the direction of the edge will be validated. If expression 22.b is fulfilled, the normal sections $\mathcal{N}_I$ and $\mathcal{N}_{II}$ behave, in practice, as straight lines.

Activity gradients usually involve processes subject to diffusion limitations, as in the case of poisons, carbonaceous deposits, or the impregnation of active agents during catalyst manufacturing. As a point at an edge constitutes a singular point for the gradient of properties subject to diffusion limitations, the restriction arising from activity gradients around the edge (eq S37 in the Supporting Information) becomes more difficult to formulate than that for the smooth sectors (eq 7.b). It is probable that if the constraint given in eq 7.b is satisfied outside the region immediately close to an edge, the specific restriction discussed in the Supporting Information will also be satisfied.

To evaluate $[\Delta M_{high}]_k$, it was assumed that very long edges and normal sections were involved. As the linear dimensions of the zones affected by the presence of an edge will be related to the penetration depth, restrictions of the following type should be additionally written down in regard to an edge k of length W_k and a normal section (generated from a point of the edge) of length L:

$$\lambda/a_k^{1/2} \ll W_k \tag{23.a}$$

$$\lambda/a_L^{1/2} \ll L \tag{23.b}$$

where a_k and a_L are suitable average activities.

In general, the restrictions discussed above should be locally satisfied at each point of each smooth sector (eqs 7), or at each point of each edge (eqs 22.a, 22.b, and 23.b). However, the integral formulation for the asymptotic regime (eqs 19−21) can still be accurately used if some of the restrictions are not strictly satisfied in relatively narrow portions of the sectors or of the edges. It will be very important to determine a value λ_M such that if $\lambda \le \lambda_M$, the asymptotic regime will apply. λ_M represents for a given catalyst a practical value satisfying the previously discussed restrictions up to a degree depending on the accuracy desired in the use of eqs 19−21. This point will be further discussed in section 6.

A final and important issue concerns the presence of vertexes on the pellet surface. We can assess the magnitude of their effect by following a similar line of reasoning as that used for edges in the previous section. Assume a vertex at which three sectors are converging, e.g., the vertex of a cube. If the penetration depth χ is small, there will be a small zone around the vertex with side length χ in which the concentration fields from the three sectors interact. Then, we cannot compute independently the reaction of the species coming from the three sectors. Hence, as a first approximation, we should subtract from eq 10 an amount corresponding to two of the sectors, i.e., $\Delta M \sim 2\chi^2 N_{AS}$. Employing eqs 8 and 14 for N_{AS} and χ, we can conclude that ΔM will be proportional to λ. As such, it will be negligible, in regard to the evaluation of M_{high}, provided that the previously discussed restrictions for λ are fulfilled.

5. Evaluation of $\omega(\theta)$

We undertake in this section the calculation of the coefficient $\omega(\theta)$ defined in eq 17.e.

The function $\omega(\theta)$ is a decreasing function of the dihedral angle θ that passes through zero at $\theta = \pi$, as depicted in Figure 3 for a first-order reaction ($r = Y$) for which the notation $\omega_1(\theta)$ is employed. (When invoking "first-order reaction" conditions, it is assumed that $\pi_A = kC_A$, that the system is isothermic, and that $\mathbf{N}_A = -D_A \nabla C_A$, with a constant D_A; hence, $Y = C_A/C_{AS}$ and $r(Y) = Y$.) When $\theta = \pi$, the external surface is actually smooth through the edge, in the sense that the vector normal to

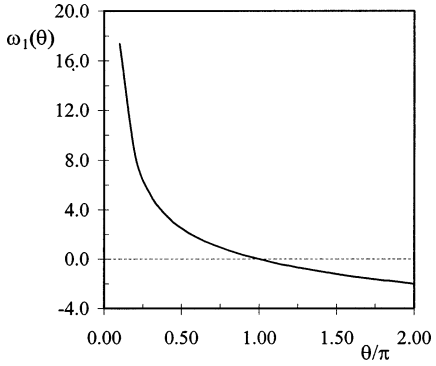

Figure 3. Plot of $\omega_1(\theta)$ [$r(Y) = Y$].

the surface is continuous. Hence, an edge with $\theta = \pi$ makes no contribution to M_{high}. For $\theta < \pi$, $\omega(\theta) > 0$ means that the edge promotes a negative contribution to M_{high} (eqs 19 and 20.a), as the flux lines from the two normal sections tend to converge, and the opposite effect is achieved when $\theta > \pi$.

The evaluation of $\omega_1(\theta)$ can be done by means of a series solution (e.g., ref 8) for eqs 17.a−c when $r(Y) = Y$. In the general case, a numerical solution should be employed, which is not a trivial task as a 2D semi-infinite medium is involved. Fortunately, the behavior of $\omega(\theta)$ turns out to be a very weak function of the form of $r(Y)$. Hence, an approximate closed expression for $\omega(\theta)$ can be developed, which will be shown to provide a quite satisfactory degree of precision for most expressions of $r(Y)$. To develop such an approximation, we have used numerical results of $\omega(\theta)$ obtained with FEMLAB v3.1 by Comsol Inc. and additional analytical information has been obtained from the behavior of $\omega(\theta)$ at angles θ close to zero and close to π, as detailed in the Appendix of this paper.

Let us first summarize the results from the Appendix. For small values of θ, the following series is shown to hold

$$\omega(\theta) = \frac{1}{\theta}(b_0 + b_1\theta^2 + b_2\theta^4 + ...) \tag{24}$$

where the dominant coefficient b_0 is given by

$$b_0 = \frac{4}{\mathscr{I}_2}\int_0^\infty [\mathscr{I}_1 - \Phi\eta_p(\Phi)]\, d\Phi \tag{25}$$

The magnitude $\eta_p(\Phi)$ is the effectiveness factor for a slab with uniform activity; that is, if $Y(\zeta)$ is the solution of $d^2Y/d\zeta^2 = \Phi^2 r(Y)$ subject to $Y(0) = 1$ and $Y'(1) = 0$, then

$$\eta_p(\Phi) = -Y'(0)/\Phi^2$$

The coefficient b_0 depends weakly on the form of $r(Y)$. For a zero-order reaction (i.e., $r = 1$ if $Y > 0$; $r = 0$ if $Y = 0$), $b_0 = 6$, and for a first-order reaction, $b_0 = 8 \ln 2 \approx 5.545$ (ratio of the values of b_0 is 1.08).

For values of around $\theta = \pi$, it is shown in the Appendix that

$$\omega(\theta) = (\pi - \theta) + o(\pi - \theta) \tag{26}$$

where $o(x)$ represents a variable such that $o(x)/x \to 0$ if $x \to 0$.

Evidently, the behavior of $\omega(\theta)$ around $\omega = \pi$ is independent of $r(Y)$.

The third point considered for developing a general expression of $\omega(\theta)$ is the value $A = -\omega(2\pi)$, that has been obtained numerically for a number of kinetic expressions. In particular, for $r = Y$, the value $A = 2$ is obtained.

Now, it has been assumed that the values b_0 and A suffice to characterize a given expression $r(Y)$, and the following correlation, which generally satisfies $\omega(\pi) = 0$, $\omega'(\pi) = -1$ (from eq 26), $\lim [\theta\ \omega(\theta)] \to b_0$ if $\theta \to 0$ (from eq 24), and $\omega(2\pi) = -A$, is proposed to evaluate $\omega(\theta)$

$$\omega(\theta) = \begin{cases} \dfrac{b_0}{\theta}\left[1 - \left(\dfrac{\theta}{\pi}\right)^{\pi^2/b_0}\right] & \text{if } 0 \le \theta \le \pi \\ \dfrac{\pi^2 A}{(\pi - A)\theta + \pi(2A - \pi)}\left[1 - \dfrac{\theta}{\pi}\right] & \text{if } \pi < \theta \le 2\pi \end{cases} \tag{27}$$

The maximum errors from eq 27 are less than 2%. In general, the second-order term in eq 20.b for η_{high} can contribute at most about 25%, for applicable values of Φ. Hence, the deviations in η_{high} introduced by using eq 27 will be well below 1%.

To obtain a completely closed formulation of $\omega(\theta)$, it is necessary to have correlations for b_0 and A.

5.1. Approximate Evaluation of b_0 and A. We have carried out numerical evaluations of both parameters in eq 27, b_0 and A, for a number of kinetic expressions $r(Y)$ that can be summarized by the general expression

$$r(Y) = e^{\delta(1-Y)}Y^n\left(\frac{1+K}{1+KY}\right)^m \tag{28}$$

For $m = 0$, values of n were tested in the range $0 \le n \le 3$. Values of $m = 1$ and 2 were used along with $n = 1$. If $\delta > 0$ (exothermic reaction effect) or $m > n$, multiple solutions may arise. The numerical experiments were restrained to values of δ and K for which multiplicity does not take place in a catalytic slab [e.g., for $(\delta, n, m) = (0, 1, 2)$ up to $K = 9$ or for $(n, m) = (2, 0)$ up to $\delta = 5$].

Values of parameter b_0 span the range $5 < b_0 < 7$; the lower values are for high reaction orders, and the higher values correspond to conditions approaching multiplicity. It was found that the values of b_0 correlate well with coefficients $\mathscr{I}_1$ and $\mathscr{I}_2$. For a given $r(Y)$, these can be straightforwardly calculated from their definitions in eqs 9. The correlation,

$$b_0 = 5.2\mathscr{I}_1^{0.3}/\mathscr{I}_2^{0.1} \tag{29.a}$$

presents an error less than 3%, and it allows the evaluation of η_{high} with an error safely below 1%.

The parameter A shows a very weak dependence on the form of $r(Y)$. The range $1.85 < A < 2.10$ encompasses all values evaluated with FEMLAB v3.1 by Comsol Inc. The following correlation allows the evaluation of A with errors below 1%:

$$A = -\omega(2\pi) = 1.9/(\mathscr{I}_1\mathscr{I}_2)^{0.07} \tag{29.b}$$

5.2. Final Assessment of the Effect of $r(Y)$ upon $\omega(\theta)$. As will be further discussed in the next section, it would have been highly desirable that $\omega(\theta)$ had been independent of $r(Y)$. From a practical point of view, however, $\omega(\theta)$ behaves as a weak function of the kinetic expression, particularly in the range $\pi/2 \le \theta \le 2\pi$. The value $\omega_1(\theta)$ for a first-order reaction can be adopted as a representative value for most kinds of kinetics. Accepting a deviation of 5% in the value of $\omega(\theta)$, we can directly employ $\omega_1(\theta)$ if either (a) $\pi/2 \le \theta \le 2\pi$ and $r(Y)$ does not lead to multiple steady states in a slab or (b) $0 \le \theta \le 2\pi$ (the full range of θ) and $5.2 \le b_0 \le 5.8$.

For power law kinetics, $r = Y^n$, the condition $5.2 \le b_0 \le 5.8$ is approximately equivalent to $^1/_3 \le n \le 3$. The specific

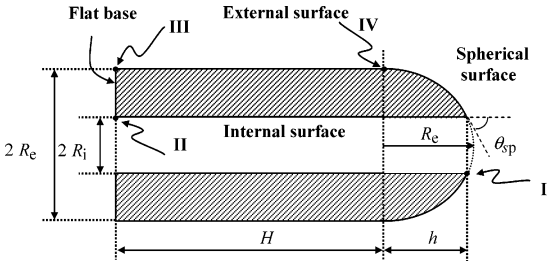

Figure 4. Sketch of a hypothetical pellet.

Table 2. Contributions to Γ for a Hollow Cylinder with a Hemispherical Head (Figure 4)

sectors	S_j	T_S	$[T_S S]_j$	fixed dimensions
external	$2\pi R_e H = 12.57$	$1/R_e = 1$	12.6	$R_e = 1$
internal	$2\pi R_i(H + h) = 9.00$	$-1/R_i = -2$	−18.0	$R_i = {}^1/_2$
spherical	$2\pi R_e h = 5.44$	$2/R_e = 2$	10.9	$H = 2$
flat base	$\pi(R_e^2 - R_i^2) = 2.36$	0	0.0	

edges	W_k	$\omega(\theta)$	$[\omega W]_k$	derived quantities
I	$2\pi R_i = 3.14$	$\omega(\pi/3) = 4.55$	14.3	$h = 0.866$ $\theta_{sp} = \pi/3$
II	$2\pi R_i = 3.14$	$\omega(\pi/2) = 2.54$	8.0	$S_p = 29.4$ $V_p = 6.07$
III	$2\pi R_e = 6.28$	$\omega(\pi/2) = 2.54$	16.0	$l = 0.206$ $\Gamma = 0.307$
IV	$2\pi R_e = 6.28$	$\omega(\pi) = 0$	0.0	
		Sum:	43.8	

approximate expression for $\omega_1(\theta)$ [$r = Y$] is derived from eq 27,

$$\omega_1(\theta) = \begin{cases} \dfrac{8 \ln 2}{\theta}\left[1 - \left(\dfrac{\theta}{\pi}\right)^{\pi^2/(8 \ln 2)}\right] & \text{if } 0 \le \theta \le \pi \\ \dfrac{2\pi^2}{(\pi - 2)\theta + \pi(4 - \pi)}\left[1 - \dfrac{\theta}{\pi}\right] & \text{if } \pi < \theta \le 2\pi \end{cases} \quad (30)$$

The exact value for the common case of $\theta = \pi/2$ is $\omega_1(\pi/2) = 8/\pi \cong 2.5465$.

5.3. Edges Separating Permeable and Sealed Sectors. Up to this point, we have considered edges between two smooth sectors belonging to S_p. Instead, if a permeable sector shares an edge with a sealed sector (belonging to S_N), the values of ω for this edge should be computed as $\omega = {}^1/_2\omega(2\theta)$, where θ is the actual angle from the intersection of both sectors. This relationship arises from considering that a sealed sector is characterized by a null flux: the same as if it were an element of symmetry. As θ can reach a maximum of (2π), it would be necessary to extend the evaluation of ω up to a hypothetical angle (4π). We have not carried out a systematic study in the range $2\pi < \theta < 4\pi$. As a point of reference, we quote that $\omega_1(3\pi) = -3.15$ [compare with $\omega_1(2\pi) = -2.0$]. A rough approximation in the range $2\pi < \theta < 4\pi$ can still be achieved by extrapolating eq 27 or 30.

5.4. Example. Figure 4 schematizes a hypothetical pellet of uniform activity consisting of a hollow cylinder with a hemispherical head. We can identify four smooth sectors corresponding to the external and internal cylindrical surfaces, the spherical zone, and the flat base. There are four circular edges: two formed from the intersection of the sphere and the internal and external cylindrical surfaces (I and IV), and two (II, III) enclosing the flat base. The contributions to Γ (eq 21.b) from those geometrical elements are displayed in Table 2.

It is worth noting some specific features: the curvature is uniform on each of the four sectors, the curvature of the internal cylinder is negative, the angle θ around each edge is uniform, and the angle around edge IV is $\theta = \pi$; hence, this edge does not contribute to Γ.

Most commercial catalytic pellets show a regular shape, and the difficulty in evaluating Γ will not be higher than that for the previous example, at least for cases of uniform activity.

Reference values of Γ for uniform activity are 0.67 (sphere), 0.5 (long circular cylinder), and 0 (slab). The body in Figure 4 (Γ = 0.31 from Table 2) is expected to behave intermediately between the case of a slab and the case of a long circular cylinder.

6. Discussion and Use of the Second-Order Expansion

We will consider first in this section the case of single reactions. Also, it will be assumed that uniform catalytic activity is involved (i.e., $a = 1$), unless specifically mentioned.

For the general case of nonlinear kinetics, the natural way to solve the problem of evaluating the effectiveness factor involves a numerical procedure. It is well-known that the difficulty in solving an equation like eq 3.a increases as λ decreases or, equivalently, as Φ increases. Villadsen and Michelsen[9] described how the global orthogonal collocation method, a very efficient procedure for 1D problems, collapses at high values of Φ. Methods based on local approximations, on the other hand, will require meshing of a size comparable to λ. This leads to a number of nodes (or elements) of the order Φ^d (d is the number of spatial coordinates in the conservation equations), if uniformly spaced. Some kind of adaptive meshing will eventually be necessary,[10] but still, there will be a high numerical cost associated with its implementation and the obvious need for a more sophisticated solver.

Therefore, it would be highly convenient to have an alternative to avoid the use of a numerical procedure at high values of Φ. In this sense, eq 20.b can be valuable for complementing the use of a numerical routine. The computational savings will be particularly relevant for 3D geometries.

As a specific example, consider a cube ($\Gamma_{cube} = \omega(\pi/2)/3$) and assume that an error of 2% is tolerable in the evaluation of η. Numerical values of η were evaluated by employing FEMLAB v3.1. For a first-order reaction ($r = Y$), the deviation between η_{high} from eq 20.b and the numerical value is −2.0% at Φ = 2.1 ($\eta_{high} = 0.380$). Defining Φ_m as the lowest Φ needed for using eq 20.b, a numerical solution will be required in this example for $\Phi < \Phi_m = 2.1$. Around 50 equally sized elements were employed by FEMLAB v3.1 (in an eighth of the cube, taking advantage of symmetry) to render an evaluation of η with an error around 2.0% at Φ = 2.1.

Instead, if we assume that the only piece of available analytical information at high values of Φ is $\eta_{limit} = \mathcal{I}_1/\Phi$ (i.e., the expression for the limiting regime), we will have to use the numerical procedure up to about Φ = 21 to keep an error of 2%. FEMLAB v3.1 employs around 100 000 equally sized elements to evaluate η at Φ = 21 with an error of 2%. Probably, this number of elements cannot be tolerated for any practical application in which the evaluation of η should be repeated many times. Of course, the use of an adaptive procedure will be beneficial in this case.

In the previous example, eq 20.b allowed one to avoid the use of the numerical procedure for values of Φ spanning 1 order of magnitude (from Φ = 2.1 to Φ = 21). In terms of changes in intrinsic kinetics, this range of Φ is equivalent to a 100-fold increase of the reaction rate coefficient.

The effect of the type of reaction rate expression can be appreciated in Table 3, where minimum values of Φ for using

Table 3. Effect of the Kinetic Expression on Minimum Values of Φ Needed for Using η_{high} (Eq 20.b) or $\eta_{limit} = \mathcal{I}_1/\Phi$ with a Tolerable Error of 2% in a Cube

$r(Y)$	Y^2	Y	1 (if $Y > 0$)	$36Y/(1+5Y)^2$
Φ_m (for η_{high})	2.10	2.10	1.53	1.30
Φ (for η_{limit})	20.5	21.0	20.8	18.5
$\Gamma = \omega(\pi/2)/3$	0.820	0.836	0.866	0.885
$\mathbb{R}$	0.49	0.50	0.47	0.41
$\mathcal{I}_1$	0.816	1	1.41	1.66

either η_{high} from eq 20.b or $\eta_{limit} = \mathcal{I}_1/\Phi$ are displayed (the same expressions as in Table 1 were used, except $r = Y^{1/2}$ for which convergence problems arose in the numerical procedure). In all cases, the parameter $\omega(\pi/2)$ for calculating Γ_{cube} was calculated from approximations 27 and 29.a. Values of $\mathcal{I}_1$ and $\mathbb{R}$ are also shown in Table 3. The span of Φ between the minimum values for using η_{high} and η_{limit} is similar for the different kinetics, and there is a beneficial trend for Φ_m to decrease as the (effective) reaction order decreases.

For the direct use of eq 20.b, as illustrated above, we should know the critical value Φ_m. To determine this value for a given problem (i.e., pellet geometry, reaction rate expression, and tolerable error), the numerical procedure can be used in an exploring initial stage. To minimize this effort (or better, to avoid it), it would be highly desirable to have some guidelines for evaluating Φ_m. At present and based on the restrictions discussed in section 4, we are trying to systematize a body of results in this direction. The majority of examples suggest that $2 < \Phi_m < 2.5$ for first-order kinetics and 2% of tolerable error, although there are geometries that promote values of Φ_m outside that range. We hope to undertake this point more amply in a separate contribution.

6.1. Use of Γ as a Shape Factor. When it is desired, or needed, to completely avoid 2D or 3D evaluations of the effective reaction rate, some kind of approximation should be introduced. A convenient approach is adopting a geometrical 1D model to approximate the behavior of a given 2D or 3D pellet. There are available in the literature some interesting proposals in this regard. The basic idea is defining a *shape factor* to characterize the geometric shape of a given catalyst and use a simple 1D geometry (the *geometric model*) holding the same value of the shape factor to compute the effective reaction rates.

A suitable 1D geometric model presenting one adjustable parameter to match the shape factor was proposed by Burghardt and Kubaczka.[11] The shape factor proposed by them to characterize 2D or 3D geometries is based on an effective diffusion length. A general procedure to evaluate this property for any pellet geometry was not given in that paper. Mariani et al.[4] employed the same geometric model but used the geometrical coefficient γ arising from the expansion of the effectiveness factor η at low values of Φ (e.g., $\eta \approx 1 - \gamma\Phi^2$, for a first-order reaction) as the shape factor. Thus, the shape factor becomes unambiguously defined for any pellet geometry. The results obtained for a single first-order reaction in hollow circular cylinders and parallelepipeds were very accurate over the whole range of Φ (maximum errors less than 1%).

Buffham[12] proposed a magnitude called *compactness* (here denoted as Q) as a shape factor:

$$Q = 1.5l(T_S)_{av} \tag{31}$$

Therefore, Q is proportional to the value of Γ in the case of uniform activity and a smooth surface (cf. eq 21.b with $\Omega_{av} = 0$). The factor 1.5 yields $Q = 1$ for a sphere. The author put forward the use of Q as a general shape factor for any kind of particulate material and application, without a specific association to the asymptotic regime in catalysts.

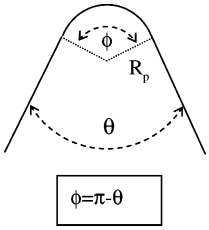

Figure 5. Cross section of a round-nose wedge.

Actually, Buffham[12] extended the use of eq 31 for geometries with flat faces (plane smooth sectors) and, therefore, straight edges (prisms, parallelepipeds, and tetrahedra).

To this end, instead of considering wedges with sharp edges (Figure 2), Buffham[12] assumed that they present a round nose in the form of a sector of a circular cylinder of radius R_p. As depicted in Figure 5, on a normal plane of such wedges, the nose meets the faces at straight angles. Hence, the cylindrical sector angle becomes defined by $\phi = \pi - \theta$.

The contribution of the lateral surface of the cylindrical sector to $(T_S)_{av}$ is

$$(T_S S)_w = (1/R_p)(\phi R_p W) = (\pi - \theta)W \tag{32}$$

where W is the length of the wedge. The radius R_p is then considered to be very small, so the lateral surface area of the cylindrical sector can be neglected in computing S_p. Considering only bodies with uniform angle θ (infinite regular prisms, parallelepipeds, and a regular tetrahedron), it follows that

$$Q = 1.5l(\pi - \theta)W_T/S_p \tag{33}$$

where W_T is the total length of the edges.

Buffham[12] compared the effectiveness factor of a first-order reaction for different catalyst geometries. Three kinds of comparisons were made. In the first case, geometries with smooth surfaces (e.g., a sphere or a very long Raschig ring) and the same Q were involved. When compared at the same value of Φ, the maximum deviation in η between the different smooth geometries was about 1%. Parallelepipeds with different aspect ratios, but with the same Q, were compared in the second case. A conclusion similar to that in the first case arose for the deviations in η. Finally, a parallelepiped and smooth geometries with the same Q were compared. In this case, the values of η for the parallelepiped showed deviations up to around 8.5% (in defect) when compared to the case of the smooth geometries, i.e., about an order of magnitude higher than in the previous cases.

These results can be explained by recalling the connection between Q and Γ. It should be stressed first that if any pair of geometries should present very close values of η for the whole range of Φ, a *necessary* condition is that the values of Γ turn out to be similar, as required by eq 20.b for high values of Φ. The first two comparisons explained above verified this requirement. The first case is rather obvious, as $Q = 1.5\Gamma$ for smooth surfaces. On the other hand, for a first-order reaction in parallelepipeds [$\theta = \pi/2$, $\omega_1(\pi/2) = 8/\pi$], $\Gamma = l(8/\pi)W_T/S_p$; then, eq 33 yields $Q = 1.5(\pi^2/4)\Gamma = 0.925\Gamma$. Thus, parallelepipeds of the same Q present the same Γ. But, a parallelepiped and a smooth catalyst showing the same value of Q will necessarily show significantly different values of Γ (the ratio is $1.5/0.925 = 1.62$), that explains the results of the third case.

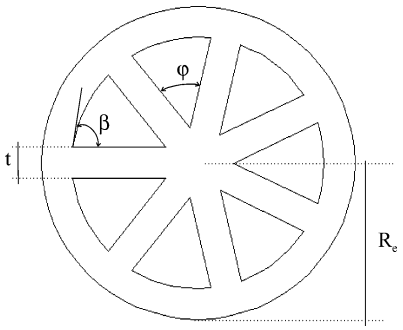

Figure 6. Cross section of a "wagon wheel" tablet.

As a further example, let us compare a long parallelepiped (P) with sides (1, 1.42, and 14.2), a sphere with an inert core (S_{IC}) with radii 0.726 and 1, and a solid sphere (S_S). P and S_{IC} have the same Q, equal to 0.617, but P and S_S have the same Γ, equal to $^2/_3$. The maximum relative deviation for η between S_{IC} and P (same Q) is 7.0% (at $\Phi \approx 1.4$), and that between P and S_S (same Γ) is 0.80% (at $\Phi \approx 1.0$).

The reason that Q is not compatible with Γ for bodies presenting edges stems from the fact that the approximation employed for the edges (eq 32) involves assuming a tiny radius of curvature ($R_p \rightarrow 0$) for the cylindrical sectors, which cannot fulfill restriction 7.a.

The appropriateness of Γ as a characteristic shape factor was also shown by Mariani et al.,[13] by fitting the adjustable parameter of the 1D geometric model of Burghardt and Kubaczka[11] with the values of Γ for several pellet shapes, including cylinders, parallelepipeds, Raschig rings, and other hollow cylinders. The values of η for a first-order reaction calculated from the 1D model differ from the actual values by no more than 1.5%.

As a specific example of the use of the 1D geometric model, consider a "wagon wheel" tablet, for which the cross section is that outlined in Figure 6, with curved and flat walls of the same thickness $t = (16/81)R_e$ (R_e is the outer radius) and a length $H = (25/27)R_e$. This tablet corresponds to the geometry of an actual commercial catalyst for the steam reforming process. Employing values of ω_1 (first-order kinetics) from eq 30, we calculate $\Gamma = 0.293$. From Figure 6, we can see that there are 14 axial edges with $\omega_1(2\pi - \beta)$, 7 axial edges with $\omega_1(2\pi - \varphi)$, and the edges of the bases (total length given by twice the perimeter of the cross section) with $\omega_1(\pi/2)$. The tablet will show a behavior somewhere between that of a slab ($\Gamma = 0$) and that of an infinitely long circular cylinder ($\Gamma = 0.5$). The free parameter of the 1D model was chosen so that the model also presents $\Gamma = 0.293$. For $r(Y) = Y$, the maximum difference between values of η from the 1D model and the actual tablet (using FEMLAB v3.1) was 0.5% (at $\Phi \approx 1.0$).

It remains to ask if Γ universally *suffices* for characterizing the catalyst shape. Keegan et al.[1] gave examples of smooth geometries, arising in monolithic reactors and presenting the same value of Γ but showing deviations between their values of η that rise well above 15%. The reason for this discrepancy was that those geometries present significantly different values of the coefficient γ representing the low Φ range. This result is not surprising: γ reflects an incipient diffusion limitation that arises from the *whole* catalyst body, while Γ reflects the diffusion limitation just in the *outer part* of the catalyst, close to S_p. Even though for a vast amount of geometries both coefficients, Γ and γ, are very strongly correlated and either of them can be used to characterize the geometrical effect, there are exceptions to the rule, as in the examples from ref 1. In these cases, the catalyst geometry should be identified by *both* coefficients, γ and Γ.

It is interesting to remark at this point that the coefficient γ is defined from the solution of a Laplace equation [$\mathcal{L}(Y) = 0$] for the actual catalyst geometry, and as such, this definition involves solving a 2D or 3D problem. Although approximate solutions have been presented for a number of practical cases,[4] it is a general conclusion that the evaluation of the coefficient Γ is considerably simpler than that of γ. Hence, when it is known that for a given type of geometry both coefficients are correlated, the use of Γ to characterize the geometry is preferred, for the sake of simplicity.

In previous paragraphs, we have referred to Γ as a shape factor. However, it should be recalled that it also depends on the activity distribution, through $(a_S^{1/2})_{av}$ and $(\mathcal{A}_S)_{av}$ (eq 19.h). Thus, Γ includes geometric and activity gradient effects, although both are clearly separable. On the other hand, we also recall that the effect of the form of $r(Y)$ cannot be separated from the edge coefficient $\omega(\theta)$. This could have been a major drawback for assigning a neat geometrical significance to Γ, but the influence of $r(Y)$ turns out to be so weak that using the value ω_1 (eq 30) will be quite satisfactory most of the time, as noted in section 5.

As a partial conclusion, there is clear evidence from single-reaction results that Γ is a significant coefficient for characterizing the catalyst shape and, as such, it can be used in connection with 1D geometrical approximations. A more detailed and systematic report in this regard is currently being prepared.

6.2. Extension to Multiple Reactions. The development in this paper and the preceding discussion were made on the basis of a single reaction. The effort of solving 2D or 3D conservation balances in multiple-reaction systems would be much more significant, in terms of implementation and computation, than that for a single reaction. It is then important to analyze how the formulation for a single reaction can be extended to multiple reactions. We do not know of other systematic studies aimed at evaluating the use of any 1D model as an approximation for complex (2D or 3D) catalyst geometries when multiple reactions occur. In view of the lack of enough background and the fact that a proper formulation would require significantly increasing the extent of the present manuscript, we will only advance here some conclusions regarding the characterization of the asymptotic regime for multiple reactions.

It was verified in the work of Keegan et al.[1] that for smooth catalyst geometries with multiple reactions the overall reaction rates depend on the same coefficient as for the single reaction, $\Gamma_{smooth} = l(T_S + \mathcal{A}_S)_{av}/(a_S^{1/2})_{av}$ (cfs. eq 19.h), provided that *all* reactions take place sufficiently close to S_p. Therefore, Γ_{smooth} can be employed, in connection to a 1D model, just as for a single reaction.

The effect of edges can be evaluated by following a similar treatment as was done for a single reaction. It is not difficult to visualize that a set of equations similar to eqs 17, but extended to all reactions, will arise. From this, a set of values $\{\omega(\theta)\}$ will come out, instead of a single value as in the case of a single reaction. Then, there will be no single coefficient Γ for the whole system but a set of values $\{\Gamma\}$ derived from the set $\{\omega(\theta)\}$. In a strict sense, this fact prevents the use of a geometric 1D model.

Nonetheless, given the fact that $\omega(\theta)$ for a single reaction was shown to vary very weakly with reaction kinetics, it can be reasonably expected that this feature will hold for multiple reaction systems. Specifically, we can expect that the value $\omega_1(\theta)$ (eq 30) will be suitable to define a single Γ to characterize the system, allowing a 1D geometric model to be defined. When

the conservation balances are linear (linear reaction rates and linear dependence of fluxes with concentration gradients), it can be shown that a single coefficient Γ defined with $\omega_1(\theta)$ strictly holds.

We can take for granted that there will be a number of multiple-reaction schemes for which the use of $\omega_1(\theta)$ and a single value of Γ will turn out to be valid, but a systematic investigation is obviously necessary to find out eventual limitations.

6.3. External Transport Limitations. The assumption of uniform state variables over S_p (assumption a in section 2) has been briefly addressed by Keegan et al.[1] It was argued that this assumption can become invalid if mass (and heat) transfer coefficients from the fluid bulk vary strongly over S_p and, simultaneously, the average impact of the external limitations is also strong. In random beds of catalytic pellets, local coefficients can indeed vary considerably, but in commercial units, the average effect will be normally minimized due to the high superficial velocities usually employed. Therefore, assumption a will be appropriate in many practical cases, but counterexamples cannot be ruled out. The whole issue is beyond the scope of this manuscript, so caution should be taken in this regard. In addition, to our knowledge, experimental information about local fluid-to-particle mass and heat transfer coefficients in packed beds is very limited. Probably, computational fluid dynamics (CFD) studies can be of great help in this regard.

7. Conclusions

The main results of this paper are eqs 19−21 expressing the effective reaction rate as a truncated series with a first-order term (proportional to Φ^{-1}) and a second-order term (proportional to Φ^{-2}) for any 2D or 3D catalyst shape. The conditions under which these expressions apply are termed the asymptotic regime. The parameter Γ (eq 19.h) defining the magnitude of the second-order correction has been obtained by adding the effect of edges to the expression previously developed for smooth surfaces.[1]

The contribution of a given edge can be evaluated by reducing the zone close to it to a straight wedge. This is a 2D problem whose relevant outcome is the coefficient $\omega(\theta)$ that depends strongly on the dihedral angle θ and weakly on the shape of the dimensionless rate $r(Y)$. A correlation for $\omega(\theta)$ applicable for most types of kinetic expressions $r(Y)$ has been presented. This correlation allows evaluating Γ in a very simple way for essentially any shape of known commercial pellets.

Basic restrictions for the settlement of the asymptotic regime have been summarized. Those arising from the existence of edges have been developed in the Supporting Information for this paper.

The expressions for the asymptotic regime can be applied straightforwardly to complement a numerical evaluation of the conservation equation. A numerical method can be employed for the relatively smooth concentration fields inside the catalyst at low values of Φ, while the asymptotic expression can be used at large values of Φ, when steep (and difficult to evaluate) solutions take place. It is shown that the lowest value of Φ for which the asymptotic expression can be used may reach 1 order of magnitude less than that when using only the first-order term (in Φ^{-1}) for the effectiveness factor.

Another important application of Γ is for fitting the adjustable parameter of a 1D geometric model intended for approximating the diffusion−reaction problem in complex 2D or 3D shapes. Γ is a characteristic coefficient enclosing the effect of geometry and activity profiles of any 2D or 3D catalytic body at high reaction rates. From the expansion of the effectiveness factor at low reaction rates, a different coefficient, γ, also encompasses geometric and activity gradient effects.[4,7] Based on previous results from Buffam,[12] Keegan et al.,[1] Mariani et al.,[4,13] and some examples provided here, it has been observed that Γ and γ are frequently very strongly correlated. In these cases, it will be more convenient to adjust the 1D geometric model with Γ, which is more easily evaluated than γ.

Even though Γ and γ are very well correlated for many types of commercial catalysts, deviations from realistic shapes have been identified. It remains to systematize these cases and propose alternatives for their approximate treatment.

A similar analysis of the asymptotic regime can be carried out for systems of multiple reactions. The presence of edges avoids, in general, the occurrence of a single value for $\omega(\theta)$ and, hence, of a single Γ. Nonetheless, considering the insensitivity of $\omega(\theta)$ with the form of the reaction rate (as proved for single reactions) and the fact that for linear systems $\omega_1(\theta)$ holds as the unique coefficient for the system, it is reasonable to expect that the value of Γ calculated with $\omega_1(\theta)$ can characterize a variety of multiple-reaction systems, similarly as it did for single reactions.

Acknowledgment

The authors wish to thank the following Argentine institutions for financial support: ANPCyT- SECyT (PICT No. 14224) and UNLP (PID No. 11/I100). N.J.M., O.M.M., and G.F.B. are Research Members of the CONICET, and S.D.K. is a fellow of the Academia Nacional de Ciencias Exactas, Físicas y Naturales.

Appendix

A.1. Solution of Eqs 17 in the Main Text around $\theta = \pi$. Equation 17.a in the main text can be rewritten in stretched Cartesian coordinates x and y (see Figure A1)

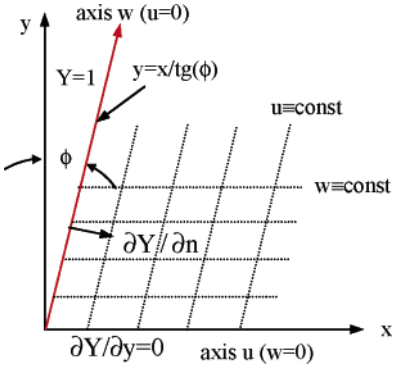

Figure A1. Coordinates to analyze the wedge at angles $\theta \approx \pi$.

$$\frac{\partial^2 Y}{\partial x^2} + \frac{\partial^2 Y}{\partial y^2} = r(Y) \qquad \text{(A1)}$$

where the axis x corresponds to the symmetry axis of the wedge and the straight line $y = x/tg(\phi)$ corresponds to one of the normal sections. Then, the boundary conditions are

$$Y = 1 \text{ at } y = x/tg(\phi); \quad \partial Y/\partial y = 0 \text{ at } y = 0$$
$$Y = 0 \text{ at } x \rightarrow \infty$$

where $\phi = (\pi - \theta)/2$, and θ is the dihedral angle, which is assumed to be close to π. Hence, ϕ will be small and positive if $\theta < \pi$ and negative if $\theta > \pi$. The derivative of Y in the

direction normal to $y = x/tg(\phi)$ can be written

$$\partial Y/\partial n = \cos(\phi)(\partial Y/\partial x)_{y=x/tg(\phi)} - \sin(\phi)(\partial Y/\partial y)_{y=x/tg(\phi)} \quad \text{(A2)}$$

The coefficient $\omega(\theta)$ in eq 17.e of the main text can now be expressed by

$$\omega(\theta) = \frac{2}{\mathscr{I}_2 \cos(\phi)} \int_0^\infty [\partial Y/\partial n + \mathscr{I}_1]\, \mathrm{d}y \quad \text{(A3)}$$

The following change of coordinates is introduced (see Figure A1),

$$w = y; \quad u = x\cos(\phi) - y\sin(\phi)$$

from which

$$\partial Y/\partial y = -\sin(\phi)\, \partial Y/\partial u + \partial Y/\partial w$$

$$\partial Y/\partial x = \cos(\phi)\, \partial Y/\partial u$$

and

$$\frac{\partial^2 Y}{\partial y^2} = \frac{\partial^2 Y}{\partial u^2}\sin^2(\phi) + \frac{\partial^2 Y}{\partial w^2} - 2\frac{\partial^2 Y}{\partial u\, \partial w}\sin(\phi);$$

$$\frac{\partial^2 Y}{\partial x^2} = \cos^2(\phi)\frac{\partial^2 Y}{\partial u^2}$$

Replacing in eq A1

$$\frac{\partial^2 Y}{\partial u^2} + \frac{\partial^2 Y}{\partial w^2} - 2\frac{\partial^2 Y}{\partial u\, \partial w}\sin(\phi) = r(Y) \quad \text{(A4)}$$

the boundary conditions become

$$\left.\begin{array}{ll} Y = 1 & \text{at } u = 0 \\ Y = 0 & \text{when } u \to \infty \end{array}\right\} \quad \text{(A5)}$$

$$\sin(\phi)\, \partial Y/\partial u = \partial Y/\partial w \text{ at } w = 0 \quad \text{(A6)}$$

From eq A2, the normal derivative on the normal section is expressed as

$$\partial Y/\partial n = (\partial Y/\partial u)_{u=0} - \sin(\phi)(\partial Y/\partial w)_{u=0}$$

Since $(\partial Y/\partial w)_{u=0} = 0$,

$$\partial Y/\partial n = (\partial Y/\partial u)_{u=0} \quad \text{(A7)}$$

Then, the integral in eq A3 becomes

$$\omega(\theta) = \frac{2}{\mathscr{I}_2 \cos(\phi)} \int_0^\infty [(\partial Y/\partial u)_{u=0} + \mathscr{I}_1]\, \mathrm{d}w \quad \text{(A8)}$$

By definition, $\sin(\phi)$ can be regarded as a small parameter in the system of eqs A4−A6. Hence, the following expansion is proposed for the solution Y:

$$Y = Y_0 + \sin(\phi)\, Y_1 + \sin^2(\phi)\, Y_2 + \ldots \quad \text{(A9.a)}$$

where Y_0, Y_1, ... are functions of u and w and do not depend on $\sin(\phi)$. Expanding $r(Y)$ around Y_0,

$$r(Y) = r(Y_0) + r'(Y_0)[\sin(\phi)\, Y_1 + \sin^2(\phi)\, Y_2 + \ldots] + {}^1/_2 r''(Y_0)[\sin(\phi)\, Y_1 + \sin^2(\phi)\, Y_2 + \ldots]^2 + \ldots \quad \text{(A9.b)}$$

Replacing eq A9.a and eq A9.b in eqs A4−A6 and collecting the terms independent of $\sin(\phi)$, the following expression is obtained:

$$\frac{\partial^2 Y_0}{\partial u^2} + \frac{\partial^2 Y_0}{\partial w^2} = r(Y_0)$$

$$Y_0 = 1 \text{ at } u = 0$$

$$\partial Y_0/\partial w = 0 \text{ at } w = 0$$

$$Y_0 = 0 \text{ when } u \to \infty$$

Due to the boundary condition $\partial Y_0/\partial w = 0$ at $w = 0$, this system reduces to

$$\frac{\mathrm{d}^2 Y_0}{\mathrm{d}u^2} = r(Y_0) \quad \text{(A10.a)}$$

$$Y_0 = 1 \text{ at } u = 0 \quad \text{(A10.b)}$$

$$Y_0 = 0 \text{ when } u \to \infty \quad \text{(A10.c)}$$

which is equivalent to expressions 11.a−c in the main text describing the limiting regime. Defining $p = \mathrm{d}Y_0/\mathrm{d}u$, eq A10.a is written

$$p(\mathrm{d}p/\mathrm{d}Y_0) = r(Y_0) \quad \text{(A11)}$$

In turn, eq 12 in the main text can be rewritten

$$p = -\mathscr{I}(Y_0)^{1/2}$$

$$\text{where } \mathscr{I}(Y_0) = 2\int_0^{Y_0} r(Y)\, \mathrm{d}Y \quad \text{(A12.a)}$$

and

$$p(0) = (\mathrm{d}Y_0/\mathrm{d}u)_{u=0} = -\mathscr{I}_1 = -[\mathscr{I}(1)]^{1/2} \quad \text{(A12.b)}$$

Collecting now terms in $\sin(\phi)$ resulting from the expansions defined in eqs A9 and taking into account the definition $p = \mathrm{d}Y_0/\mathrm{d}u$,

$$\frac{\partial^2 Y_1}{\partial w^2} + \frac{\partial^2 Y_1}{\partial u^2} - r'(Y_0)Y_1 = 0 \quad \text{(A13.a)}$$

$$Y_1 = 0 \text{ at } u = 0; \quad \partial Y_1/\partial w = p \text{ at } w = 0; \quad Y_1 = 0 \text{ when } u \to \infty \quad \text{(A13.b)}$$

Before attempting a solution for Y_1 from eqs A13, it is convenient to express $\omega(\theta)$, eq A8, according to expansion A9.a. Considering eq A12.b, we can write

$$\omega(\theta) = \frac{2tg(\phi)}{\mathscr{I}_2} \int_0^\infty [\partial Y_1/\partial u]_{u=0}\, \mathrm{d}w + o(\sin\phi)$$

and because ϕ is small,

$$\omega(\theta) = \frac{(\pi - \theta)}{\mathscr{I}_2} \int_0^\infty [\partial Y_1/\partial u]_{u=0}\, \mathrm{d}w + o(\pi - \theta) \quad \text{(A14)}$$

Hence, our target is now finding an expression for the integral in eq A14. It will become apparent that this integral can be directly evaluated by appropriately manipulating eqs A13, without the need of knowing the field Y_1.

To this end, we should first recall from the main text that far from the influence of the edge (i.e., at high values of w) the solution Y_0 of the limiting regime holds. As a consequence, Y_1

and its derivates vanish at high values of w. In particular,

$$\partial Y_1/\partial w = 0 \text{ if } w \rightarrow \infty \qquad \text{(A15.a)}$$

On the other hand, we should also recall that the solution Y_0 varies monotonically with u. Hence, both variables, Y_0 and u, can be exchanged, according to convenience. In particular, partial derivatives with respect to u (for fixed values of w) can be expressed as partial derivatives with respect to Y_0. Then, the following relation will be employed,

$$\frac{\partial^2 Y_1}{\partial u^2} - r'(Y_0)Y_1 = \frac{\partial \Psi}{\partial Y_0} \qquad \text{(A15.b)}$$

where

$$\Psi = p\left(\frac{\partial Y_1}{\partial u} - \frac{dp}{dY_0} Y_1\right) \qquad \text{(A15.c)}$$

Equation A15.b can be checked by performing the derivative of the right-hand term, recalling the definition $p = dY_0/du$ and eq A11. Equation A13.a can now be written as

$$\frac{\partial \Psi}{\partial Y_0} + \frac{\partial^2 Y_1}{\partial w^2} = 0$$

Integrating over variable Y_0, from $Y_0 = 0$ to $Y_0 = 1$ (equivalently, from $u \rightarrow \infty$ to $u = 0$), and recalling that Y_0 and w are independent variables:

$$\int_{u=\infty}^{u=0} d\Psi + \frac{\partial^2}{\partial w^2}\int_0^1 Y_1\, dY_0 = \Psi|_{u=0} - \Psi|_{u\rightarrow\infty} + \frac{\partial^2}{\partial w^2}\int_0^1 Y_1\, dY_0 = 0$$

As $Y_1 = 0$ at $u = 0$, $\Psi|_{u=0} = p(0)(\partial Y_1/\partial u)_{u=0}$ (see eq A15.c). Besides $\Psi|_{u\rightarrow\infty} = 0$, as for $u \rightarrow \infty$, $p \rightarrow 0$. By replacing these terms and introducing $\partial/\partial w$ under the integral, the following relationship is obtained:

$$p(0)(\partial Y_1/\partial u)_{u=0} + \frac{\partial}{\partial w}\int_0^1 (\partial Y_1/\partial w)\, dY_0 = 0$$

This expression is now integrated over w, from $w = 0$ to w $\rightarrow \infty$,

$$p(0)\int_0^\infty (\partial Y_1/\partial u)_{u=0}\, dw + [\int_0^1 (\partial Y_1/\partial w)\, dY_0]_{w\rightarrow\infty} - [\int_0^1 (\partial Y_1/\partial w)\, dY_0]_{w=0} = 0$$

The integral evaluated at $w \rightarrow \infty$ is nil (eq A15.a), and replacing $\partial Y_1/\partial w = p$, at $w = 0$ (eqs A13.b),

$$p(0)\int_0^\infty (\partial Y_1/\partial u)_{u=0}\, dw = \int_0^1 p\, dY_0$$

Finally, considering eqs A12 for p and $p(0)$ and the definition of $\mathscr{I}_2$ in eq 9.c in the main text,

$$(-\mathscr{I}_1)\int_0^\infty \left(\frac{\partial Y_1}{\partial u}\right)_{u=0} dw = -\mathscr{I}_1\mathscr{I}_2$$

Replacing the integral

$$\int_0^\infty \left(\frac{\partial Y_1}{\partial u}\right)_{u=0} dw$$

in eq A14, we obtain for $\omega(\theta)$

$$\omega(\theta) = (\pi - \theta) + o(\pi - \theta) \qquad \text{(A16)}$$

A.2. Solution of Eqs 17 in the Main Text for Small Angles θ. If θ is close to zero, the flux in the angular direction φ of the polar coordinates employed in eqs 17 of the main text will be dominant with respect to the flux in the radial direction ρ, at least at points sufficiently far from the edge. Thus, at a given radius ρ (not so small), Y will primarily depend on the generic arc length ($\rho\varphi$) measured from $\varphi = 0$ and on the total arc length ($\rho\theta/2$), where the symmetry condition applies. Based on this observation, the following expansion is proposed for the solution of Y at small values of θ

$$Y = Y_0 + \frac{1}{\rho^2}Y_1 + \frac{1}{\rho^4}Y_2 + \frac{1}{\rho^6}Y_3 + ... \qquad \text{(A17)}$$

where

$$Y_i = Y_i(s; \varsigma) \text{ for } i = 0, 1, 2, ... \text{ with } s = \rho\varphi \text{ and } \varsigma = \rho\theta/2$$

Expanding $r(Y)$ around Y_0,

$$r(Y) = r(Y_0) + r'(Y_0)\left(\frac{1}{\rho^2}Y_1 + \frac{1}{\rho^4}Y_2 + ...\right) + \frac{1}{2}r''(Y_0)\left(\frac{1}{\rho^2}Y_1 + \frac{1}{\rho^4}Y_2 + ...\right)^2 + ... \qquad \text{(A18)}$$

Considering the boundary conditions $Y = 1$ at $\varphi = 0$ and $\partial Y/\partial\varphi = 0$ at $\varphi = \theta/2$, we obtain for the functions Y_i in eq A17

$$Y_0 = 1 \text{ at } s = 0; \quad \partial Y_0/\partial s = 0 \text{ at } s = \varsigma \qquad \text{(A19.a)}$$

$$Y_i = 0\ (i = 1, 2, ...) \text{ at } s = 0; \quad \partial Y_i/\partial s = 0 \text{ at } s = \varsigma \qquad \text{(A19.b)}$$

Replacing eqs A17 and A18 in eq 17.a of the main text and collecting terms that contain powers ρ^{-2i} ($i = 0, 1, 2, ...$),

$$i = 0: \quad \partial^2 Y_0/\partial s^2 = r(Y_0) \qquad \text{(A20.a)}$$

$$i = 1: \quad \mathscr{L}_0(Y_0) + \partial^2 Y_1/\partial s^2 = Y_1 r'(Y_0) \qquad \text{(A20.b)}$$

$$i = 2: \quad \mathscr{L}_1(Y_1) + \partial^2 Y_2/\partial s^2 = Y_2 r'(Y_1) + \frac{1}{2}Y_1 r''(Y_0), \text{ etc.} \qquad \text{(A20.c)}$$

where the operator $\mathscr{L}_i$ ($i = 0, 1, 2, ...$) is defined by $\mathscr{L}_i = (2i)^2 + (1 - 4i)\mathscr{P} + \mathscr{P}^2$ and $\mathscr{P} = s(\partial/\partial s) + \varsigma(\partial/\partial\varsigma)$.

It is recalled that the functions $Y_i(s; \varsigma)$ only depend on one spatial coordinate (s) and on a parameter (ς), so the boundary conditions (eqs A19) and conservation balances (eqs A20) actually describe 1D variations of Y_i (on s) at a given value of ς. Hence, a proper interpretation should be given to the partial derivatives in eqs A19 and A20 and in the definition of the operator $\mathscr{P}$.

The coefficient $\omega(\theta)$ in eq 17.e of the main text is now expressed

$$\omega(\theta) = \frac{2}{\mathscr{I}_2}\int_0^\infty [(\partial Y/\partial s)_{s=0} + \mathscr{I}_1]\, d\rho = \frac{2}{\mathscr{I}_2}\int_0^\infty [(\partial Y_0/\partial s)_{s=0} + \mathscr{I}_1]\, d\rho + \frac{2}{\mathscr{I}_2}\sum_{i=1}^{\infty}\int_0^\infty \rho^{-2i}(\partial Y_i/\partial s)_{s=0}\, d\rho$$

The derivatives $(\partial Y_i/\partial s)_{s=0}$ depend only on ς. Replacing $\rho = (2/\theta)\varsigma$ and $d\rho = (2/\theta)\, d\varsigma$, we obtain

$$\omega(\theta) = \frac{1}{\theta}(b_0 + b_1\theta^2 + b_2\theta^4 + ...) \qquad \text{(A21)}$$

where

$$b_0 = \frac{4}{\mathscr{T}_2}\int_0^\infty [(\partial Y_0/\partial s)_{s=0} + \mathscr{T}_1]\, d\varsigma \qquad \text{(A22.a)}$$

$$(i \geq 1) \qquad b_i = \frac{4^{(1-i)}}{\mathscr{T}_2}\int_0^\infty (\partial Y_i/\partial s)_{s=0}\varsigma^{-2i}\, d\varsigma \qquad \text{(A22.b)}$$

The coefficients b_i ($i = 0, 1, 2, ...$) depend only on the form of $r(Y)$.

We are specifically interested in the coefficient b_0, for which the solution Y_0 of eq A20.a and boundary conditions A19.a corresponds to the solution in a catalytic slab with uniform activity and width (2ς). The Thiele modulus for this slab is simply $\Phi = \varsigma$. By denoting $\eta_p(\Phi)$ as its effectiveness factor, we can write

$$b_0 = \frac{4}{\mathscr{T}_2}\int_0^\infty [\mathscr{T}_1 - \Phi\eta_p(\Phi)]\, d\Phi \qquad \text{(A23)}$$

Supporting Information Available: Figures, equations, and discussion describing the validation of the straight-wedge approach accounting for the effect of edges. This material is available free of charge via the Internet at http://pubs.acs.org.

Nomenclature

$\mathscr{A}_S$ = coefficient defined in eq 6.a [dimensionless]
a = catalytic activity [dimensionless]
a_S = local catalytic activity on S_p [dimensionless]
C_A = molar concentration of reactant A [mol m^{-3}]
$\mathscr{T}_1$ = coefficient defined in eq 9.b [dimensionless]
$\mathscr{T}_2$ = coefficient defined in eq 9.c [dimensionless]
$\mathscr{J}_A$ = coefficient defined in eq 2.b [mol m^{-1} s^{-1}]
$l = V_p/S_p$, characteristic length [m]
$\mathscr{L}$ = Laplacian operator [m^{-2}]
M = overall consumption rate [mol s^{-1}]
$\mathbf{n}$ = normal unit vector on S_p [dimensionless]
$\mathscr{N}_I, \mathscr{N}_{II}$ = normal sections from the plane normal to the edge
$\mathbf{N}_A$ = molar flux of reactant A [mol m^{-2} s^{-1}]
$\mathbb{R} = \mathscr{T}_2/\mathscr{T}_1$ [dimensionless]
R = radial coordinate [m]
R_a, R_b = principal radii of curvature [m]
$r(Y) = \pi_A(Y)/\pi_{AS}$, relative reaction rate [dimensionless]
S_N = external surface area of the catalytic body inaccessible to reactants [m^2]
S_p = external surface area of the catalytic body accessible to reactants [m^2]
S_j = area of the jth smooth sector [m^2]
T_S = sum of local principal curvatures on S_p defined in eq 5 [m^{-1}]
V_p = volume of the catalytic body [m^3]
W_k = length of kth edge [m]
Y = concentration defined in eq 2.a [dimensionless]

Greek Letters

γ = geometric coefficient [dimensionless]
Γ = coefficient defined in eq 19.h [dimensionless]
λ = global reaction scale defined in eq 3.d [m]
$\lambda_S = \lambda/a_S^{1/2}$, local reaction scale at S_p [m]
π_A = specific consumption rate of reactant A [mol m^{-3} s^{-1}]
$\Phi = l(\pi_{AS}/\mathscr{J}_A)^{1/2}$, Thiele modulus [dimensionless]
η = effectiveness factor [dimensionless]
ξ_n = coordinate along the inward normal to S_p
$\zeta = \xi_n/\lambda_S$, stretched coordinate [dimensionless]
χ = penetration depth [m]
$\omega(\theta)$ = parameter defined in eq 17.e
θ = dihedral angle defined by the tangents of $\mathscr{N}_I$ and $\mathscr{N}_{II}$ at the edge

Subscripts

e = chemical equilibrium
high = asymptotic regime
limit = limiting regime
S = value at S_p

Literature Cited

(1) Keegan, S. D.; Mariani, N. J.; Martínez, O. M.; Barreto, G. F. Behavior of smooth catalysts at high reaction rates. *Chem. Eng. J.* **2005**, *110*, 41.

(2) Papadias, D.; Edsberg, L.; Björnbom, P. Simplified method for effectiveness factor calculations in irregular geometries of washcoats. *Chem. Eng. Sci.* **2000**, *55*, 1447.

(3) Keegan, S. D.; Mariani, N. J.; Bressa, S. P.; Mazza, G. D.; Barreto, G. F. Approximation of the Effectiveness Factor in Catalytic Pellets. *Chem. Eng. J.* **2003**, *94*, 107.

(4) Mariani, N. J.; Keegan, S. D.; Martínez, O. M.; Barreto, G. F. A One-Dimensional Equivalent Model to Evaluate Overall Reaction Rates in Catalytic Pellets. *Chem. Eng. Res. Des.* **2003**, *81* (Part A), 1033.

(5) Gonzo, E. E.; Gottifredi, J. C. Rational Approximation of Effectiveness Factor and General Diagnostic Criteria for Heat and Mass Transport Limitations. *Catal. Rev.—Sci. Eng.* **1983**, *25*, 119.

(6) Wedel, S.; Luss, D. A Rational Approximation of the Effectiveness Factor. *Chem. Eng. Commun.* **1980**, *11*, 245.

(7) Aris, R. *The Mathematical Theory of Diffusion and Reaction in Permeable Catalysts*; Oxford University Press: London, 1975.

(8) Carslaw, H. S.; Jaeger, J. C. *Conduction of Heat in Solids*, 2nd ed.; Oxford University Press: Oxford, 1959.

(9) Villadsen, J.; Michelsen, M. L. *Solution of differential equation models by polynomial approximation*; Prentice Hall Inc.: Upper Saddle River, NJ, 1978.

(10) Bressa, S. P.; Mariani, N. J.; Ardiaca, N. O.; Mazza, G. D.; Martínez, O. M.; Barreto, G. F. An Algorithm for Evaluating Reaction Rates of Catalytic Reaction Networks with Strong Diffusional Effects. *Comput. Chem. Eng.* **2001**, *25*, 1185.

(11) Burghardt, A.; Kubaczka, A. Generalization of the Effectiveness Factor for Any Shape of a Catalyst Pellet. *Chem. Eng. Process.* **1996**, *35*, 65.

(12) Buffham, B. A. The size and compactness of particles of arbitrary shape: application to catalyst effectiveness factors. *Chem. Eng. Sci.* **2000**, *55*, 5803.

(13) Mariani, N. J.; Keegan, S. D.; Martínez, O. M.; Barreto, G. F. Ajuste de un Modelo Uni-dimensional Equivalente para Analizar Pastillas Catalíticas de Forma Arbitraria. *Actas del XIII Congreso Argentino de Catálisis y II Congreso Mercosur de Catálisis*; **2003**, *112*, 1.

Received for review June 21, 2005
Revised manuscript received October 19, 2005
Accepted October 21, 2005

IE050740M